

**TNF Receptor Associated Periodic Syndrome associated with gonosomal mosaicism of a novel 24 nucleotide *TNFRSF1A* deletion**

Dorota M Rowczenio<sup>1</sup>, Hadija Trojer<sup>1</sup>, Egun Omoyinmi<sup>2</sup>, Juan I. Aróstegui<sup>3</sup>, Grigor Arakelov<sup>4</sup>, Anna Mensa-Vilaro<sup>3</sup>, Anna Baginska<sup>1</sup>, Caroline Silva Pilorz<sup>1</sup>, Guosu Wang<sup>5</sup>, Thirusa Lane<sup>1</sup>, Paul Brogan<sup>2</sup>, Philip N Hawkins<sup>1</sup> and Helen J Lachmann<sup>1</sup>

<sup>1</sup>National Amyloidosis Centre, Centre for Amyloidosis and Acute Phase Proteins, Division of Medicine, Royal Free Campus, UCL, Rowland Hill Street, London, UK

<sup>2</sup>Institute of Child Health, UCL, London, UK

<sup>3</sup>Department of Immunology. Hospital Clinic-IDIBAPS. Barcelona. Spain

<sup>4</sup>Group for Bioinformation Technologies of Research Centre for Critical Technologies, Russian-Armenian Slavonic University, Yerevan, Armenia

<sup>5</sup>Infectious Disease and Microbiology Unit, Institute of Child Health, UCL, London, UK

Dr Omoyinmi is supported by Rosetrees, and in part by SOBI, who also provided grant funding for the next generation sequencing experiments reported in this manuscript. There is no other financial support or other benefits from commercial sources for the work reported on in this manuscript, or any other financial interests that any of the authors may have, which could create a potential conflict of interest or the appearance of a conflict of interest with regard to the work.

This article has been accepted for publication and undergone full peer review but has not been through the copyediting, typesetting, pagination and proofreading process which may lead to differences between this version and the Version of Record. Please cite this article as an 'Accepted Article', doi: 10.1002/art.39683

© 2016 American College of Rheumatology

Received: Jun 17, 2015; Revised: Feb 16, 2016; Accepted: Mar 10, 2016

This article is protected by copyright. All rights reserved.

**Abstract**

**Objective:** To investigate the molecular cause of persistent fevers in a patient returning from working overseas, in whom investigations for tropical diseases were negative.

**Methods:** DNA was extracted from whole blood, leukocyte subpopulations, saliva, hair root and sperm. The *TNFRSF1A* gene was analysed by polymerase chain reaction (PCR), allele specific (AS)-PCR, Sanger-sequencing and, next-generation sequencing. *In silico* molecular modelling was performed to predict the structural and functional consequences to the extracellular domain of the mutant TNFR1 protein.

**Results:** Sanger sequencing corroborated by AS-PCR detected a novel in-frame deletion of 24 nucleotides (c.255\_278del) in the *TNFRSF1A* gene which was subsequently confirmed by the next-generation sequencing methods (targeted sequencing and amplicon-based deep sequencing). The latter revealed variable frequency of the mutant allele among different cell lines including sperm, supporting the presence of gonosomal *TNFRSF1A* mosaicism. The patient had a complete response to treatment with IL-1 blockade, with resolution of symptoms and normalization of acute phase proteins.

**Conclusion:**

We describe the first case of gonosomal *TNFRSF1A* mosaicism in TRAPS due to a novel, somatic 24 nucleotide in-frame deletion. The clinical picture including complete response to IL-1 blockade were typical for TRAPS. This case adds TRAPS to the list of dominantly inherited autoinflammatory diseases reported to be caused by somatic (or postzygotic) mutation.

## Introduction

TNF Receptor - Associated Periodic Syndrome (TRAPS) is an autosomal dominant disease caused by gain-of-function mutations in the TNF superfamily receptor 1A (*TNFRSF1A*) (1) gene encoding the 55 kDa TNF receptor type I (TNFR1). TRAPS was initially described in 1982 in an Irish-Scottish family with a 'periodic disease' complicated by AA amyloidosis (2). Subsequently it has been reported in different ethnic groups including Caucasians, Black Americans, Japanese and subjects of Mediterranean ancestry (3-5). The disease is characterized by episodes of fever accompanied by severe abdominal pain, arthralgia, migratory myalgia, rash, chest pain, lymphadenopathy, ocular inflammation, and periorbital swelling. The duration of the attacks can range from a few days to several weeks or more, with onset from early childhood to adulthood. During febrile episodes, patients with TRAPS demonstrate elevation of C-reactive protein (CRP) and serum amyloid A protein (SAA) and are at high risk of developing AA amyloidosis (6, 7).

TNFR1 belongs to a death domain superfamily and contains an extracellular motif containing four cysteine-rich domains (CRDs), a transmembrane domain, and an intracellular death domain. Binding of TNF $\alpha$  to the extracellular region of TNFR1 results in trimerisation of the receptor and activation of NF-kappa B, leading to either inflammation or apoptosis. The mechanisms by which over 100 mutations in *TNFRSF1A* gene induce TRAPS remains to be fully elucidated, but are currently thought to be largely associated with endoplasmic reticulum stress due to retention of misfolded protein (8). It is well recognised that the disease phenotype varies with respect to the age at disease onset, duration and severity of the febrile episodes as well as risk of developing AA amyloidosis (7). Although earlier series suggested that mutations affecting extracellular cysteine residues and the p.T50M variant were associated with more severe disease and a higher risk of serious complications, this has not been supported by the recent large Eurofevers series (7).

Here we report a patient with the TRAPS phenotype, in whom we identified a novel 24 nucleotide in frame deletion in the *TNFRSF1A* gene. The mutant allele frequency (MAF) varied among different cell populations, including sperm, indicating findings consistent with gonosomal *TNFRSF1A* mosaicism. IL-1 blockade is the most effective therapy for most patients with TRAPS, and the patient responded completely to this treatment further corroborating the disease phenotype.

## Materials and Methods

### Case report

A 41 year old British man from non-consanguineous kindred with a history of recurrent fevers was referred to our clinic by an infectious diseases unit. He had presented after a period working in Asia and an extensive work up had demonstrated persistent inflammatory disease but no underlying infectious or autoimmune cause. On direct questioning he described previously undisclosed symptoms from early adolescence, including an appendectomy at the age of 12 in the context of severe abdominal pain. Since then he had had 10 to 12 attacks of severe abdominal pain per year. These lasted approximately two weeks usually starting in either loin and migrating to the front of his abdomen. Other attack features included pleuritic chest pain, headache, arthralgia, myalgia, night sweats, generalised erythema and unilateral painless cervical lymphadenopathy. He had occasional red eyes but no periorbital oedema or periorbital pain. He was of normal population height, but significantly shorter than his siblings and had a late onset of puberty at 16 years of age. He reported that his attacks could be triggered by stress, cold, physical exercise and in some cases diet. Despite that, he was physically extremely fit and in full time employment. He had never received anti-inflammatory treatment. On examination he had bilateral red eyes and a generalised erythematous rash particularly across his chest. He was tender over his left loin

with no features of peritonism, nor evidence of arthritis. He had minor cervical lymphadenopathy. His inflammatory markers were extremely elevated with SAA 258 mg/L (normal range <10mg/l) and CRP 87 mg/L (normal range <10mg/l). His three siblings, parents and four children denied any similar symptoms. His clinical picture was consistent with TRAPS (7), thus genetic testing was performed.

## **Methods**

### **Isolation of DNA**

DNA was extracted from whole blood, saliva, hair root and sperm using QIAamp DNA Investigator Kit (Qiagen, Velno, The Netherlands) according to the manufacturer's protocol.

In addition 20 ml of fresh whole blood was collected into EDTA tubes for isolation of T lymphocytes, B lymphocytes, monocytes and neutrophils using magnetic nanoparticles (Stemcell Technologies, Inc., Manchester, UK) following the manufacturer's protocol. Purity of each cell subpopulation was determined by flow cytometry and was always >98% (data not shown).

### **PCR and Sanger sequencing of *TNFRSF1A***

*TNFRSF1A* gene (NCBI Reference Sequence: NM\_001065.3) exons 2 to 7 and introns 2, 4 and 6 was amplified by PCR and sequenced with Big Dye Terminator v 3.1 Ready Reaction Cycle Sequencing kit (Applied Biosystems, Warrington, UK). The electropherograms were analysed on the ABI 3130xl Genetic Analyser using Sequencing Analysis Software version 5.4.

### **Allele-specific PCR of *TNFRSF1A***

Allele-specific (AS) PCR is used to discriminate between the wild type and mutant alleles relying on the complementarity of the primers. For *TNFRSF1A* gene forward wild type (5'-GTGTGAGAGCGGCTCCT-3') and forward mutant (5'-CTGCAGGGAGTGTGAAAAC-3') primers were designed. Their sequence was complementary to, and would only amplify the wild type and the mutant allele respectively (Figure 1D). DNA was amplified in two separate reactions using HotStarTaq DNA Polymerase Kit (Qiagen, Velno, The Netherlands): reaction 1 contained wild type primer and reaction 2 contained mutant primer, other reagents including the common reverse primer (5'-AACACACACCTTCCTGCC-3') were identical in both reactions. The following cycling conditions were used: initial denaturation at 94°C for 15 minutes, then 35 cycles consisting of denaturation at 94°C for 45 seconds, annealing at 60°C for 45 seconds and extension at 72°C for 1 minute, followed by a single cycle of 72°C for 10 minutes. The two amplicons containing wild type and mutant alleles were sequenced with a common reverse primer.

#### **Next-generation sequencing studies**

A targeted panel containing 19 genes associated with monogenic autoinflammatory diseases (Table 1 in Supplemental data) was used to confirm the *TNFRSF1A* deletion and to search for other pathogenic variants. DNA was isolated from whole blood and amplified using the Agilent SureSelect Target Enrichment system. The QXT library generated from 50ng DNA input was sequenced on Illumina MiSeq platform. Data analysis was performed using the Galaxy Web-based suite as previously described (9).

The MAF was established by amplicon-based deep sequencing (ADS) on DNA isolated from T lymphocytes, B lymphocytes neutrophils, monocytes, saliva, hair root and sperm. The amplicons of each DNA sample were obtained using a conventional PCR amplification, with the appropriate tags to identify each sample and sequenced on an IonTorrent platform.

### Homology modeling of TNFR1 extracellular domain

Detailed comparison of the native and variant TNFR1 proteins was performed by *in silico* molecular modeling focusing on the extracellular domain affected by the deletion. As a template we used the crystal structure of 1TNR (10) obtained from Protein Data Bank (online at <http://www.rcsb.org/pdb/>). The tertiary structure of the mutant TNFR1 was predicted from this template with ROSETTA 3.5 software (11); accuracy and resolution of the model was obtained with VADAR (12) and RESPROX (13) software. The quality and stereochemical correctness of the mutated receptor was assessed by Ramachandran plot. Mutated and native proteins were subjected to 20,000 steps of Steepest Descent (SD) minimization algorithm and to 40,000 steps of Adopted Basis Newton-Raphson (ABNR) minimization algorithm. Visualization and analysis of each model were performed with VMD 1.9.2 program (14).

## Results

### Sanger sequencing, allele-specific (AS) PCR

Sanger sequencing performed on DNA isolated from whole blood revealed an abnormal electropherogram in the exon 3 in the *TNFRSF1A* gene with the fluorescence peaks representing the mutant allele greatly reduced in comparison to wild type allele; nonetheless the sequence was suggestive of a large deletion (Figure 1A).

Allele-specific (AS) PCR followed by Sanger sequencing of the specific amplicons revealed the c.255\_278 deletion resulting in a novel in frame deletion of eight amino acids (p.Ser86\_Glu93del according HGVS nomenclature recommendations, and p.Ser57\_Glu64del according the 'initial' nomenclature as used in the Infervers database) (Figure 1B and 1C).

Analysis of parental DNA by both Sanger and AS PCR revealed wild type *TNFRSF1A* genotype.

### Next-generation sequencing studies

Targeted sequencing confirmed the presence of the *TNFRSF1A* p.Ser86\_Glu93 deletion (Figure 1E); no other pathogenic variants were found among the panel of 19 autoinflammatory genes tested in our patient. The frequency of the mutant allele detected by amplicon-based deep sequencing in different cell subpopulations is displayed in Figure 1F.

### ***In silico* molecular modeling**

Comparing the topology of extracellular domains of the wild type and the mutant TNFR1 we determined that the p.Ser86\_Glu93 deletion resulted in lengthening of the mutated peptide from 66.90 Å (for the native) to 85.94 Å. The deletion reduced the minimization energy of the mutant receptor by 168 Kcal/mol compared to 1432 Kcal/mol in the wild type. Furthermore this mutation leads to numerous structural rearrangements (Supplement, Figure 1), which result in changes of the protein surface profile, including shifts in the composition and structure of the three ligand-receptor binding pockets: p.Glu85\_Cys102; p.Arg106\_Gly110 and p.Trp136\_Cys143 (Figure 2). The first of these three includes the residues p.Ser86\_Glu93 which are deleted by the mutation.

### **Treatment**

The patient commenced treatment with s.c. anakinra (100 mg/day), to which he had a dramatic response with a resolution of all symptoms within 24 hours and normalization of SAA and CRP from median pre-treatment values of 171 mg/L and 35 mg/L to 8.1 mg/L and 4 mg/L respectively. There was no adverse reaction to treatment and the patient has had sustained complete remission for 3.5 years on anakinra 100 mg administered on alternate days. Remarkably, this treatment period includes three months on a charitable race to the South Pole (Figure 3).

### **Discussion**

We report the first case of TRAPS caused by a *de novo* mosaic deletion in the *TNFRSF1A* gene. The *TNFRSF1A* gene is located on chromosome 12p13 comprising 10 exons (1). Over 100 pathogenic TRAPS causing mutations have been identified and most are single nucleotide substitutions (95%), although deletions and insertions have also been reported (15). One such example is the c.586\_612del27 in-frame deletion of 27 nucleotides in exon 6, resulting in p.Leu196\_Gly204del, found in a 22 year old man originating from Mauritius, who suffered with fever, severe abdominal pain and lymphadenopathy (16). His disease onset was at the age of 2 years, which rapidly progressed to amyloidosis with severe renal impairment requiring dialysis from age 19 years. His brother also suffered with AA amyloidosis and underwent renal transplantation at the age of 32 years (16).

The novel mutation identified in our patient (c.255\_278del) results in a deletion of eight amino acids p.Ser86\_Glu93del from the cysteine-rich domain 2 (CRD2) (Figure 2), and is the second largest deletion reported in the *TNFRSF1A* gene. CRD2 consists of 41 amino acids and residues from Ser86 to Phe89 are structurally highly conserved (10). In particular, the hydrophobic Phe89 residue plays a crucial role in proper CRD2 folding, since its side chain stabilizes the structure by interacting with both the second disulfide bridge (formed between Cys102 and Cys117) and the Ser-103-Asp-122 hydrogen bond bridge (10). Using *in silico* analyses we were able to show that the deletion introduces dramatic structural changes to the tertiary structure of TNFR1 extracellular domain including shifts of the receptor-ligand binding pockets.

Mosaicism is characterized by presence of at least two genetically distinct populations of cells within one organism, arising from a post-zygotic mutation, and is well described in cancer and neurodegenerative diseases (17). Such *de novo* post-zygotic mutations may occur at any stage from early embryogenesis through adult life, and in the latter are likely to present in only restricted cell lines. Advances in sequencing have demonstrated that somatic

mosaicism is a feature of a number of dominantly inherited systemic autoinflammatory diseases, particularly in cryopyrin associated periodic fever syndrome (CAPS). Historically almost 50% of children with the most severe CAPS were ‘mutation negative’ by conventional Sanger sequencing, but it is now clear that up to 70% of such patients carry mosaic variants (9, 18, 19). A recent publication describes somatic *NOD2* mosaicism causing Blau syndrome (20), another dominant autoinflammatory disease.

The patient here described represents the first report of gonosomal *TNFRSF1A* mosaicism in TRAPS. The 24 nucleotides deletion was detected in all tissues studied, including sperm, at varying frequencies from 4% to 30% (Figure 1). The presence of the variant sequence in all cell lines indicates that the mutational event must have occurred at the very early stages of embryogenesis, probably during the pluripotent stage. Our patient’s parents were asymptomatic and both had wild-type *TNFRSF1A* genotypes sequence (data not shown), confirming that the mutation occurred *de novo*. Almost certainly it is the mutation in the hematopoietic cells which are responsible for the clinical symptoms in our patient. As predicted for TRAPS he has achieved a complete clinical and serological response to IL-1 blockade with anakinra. Importantly, the finding of a mutant allele frequency of 16% in his sperm raises the possibility of heritable disease and highlights the importance of discussing possible risks to offspring.

### **Conclusion**

We describe a patient with TRAPS in whom we found a novel in-frame 24 nucleotide deletion by Sanger sequencing and AS-PCR. Next generation sequencing analyses revealed the post-zygotic nature of this novel mutation, and the studies of body distribution confirmed the first known case of gonosomal *TNFRSF1A* mosaicism. Although proving pathogenicity of a novel mutation in a single case is challenging particularly in the absence of clear

functional consequences, extensive corroborative data including sequencing a panel of 19 autoinflammatory genes and *in silico* modelling strongly suggest that this mutation is disease causing. Supporting this basic data, the symptoms and response to IL-1 blocking treatment were completely typical for TRAPS.

Accepted Article

**References:**

1. McDermott MF, Aksentijevich I, Galon J, McDermott EM, Ogunkolade BW, Centola M, et al. Germline mutations in the extracellular domains of the 55 kDa TNF receptor, TNFR1, define a family of dominantly inherited autoinflammatory syndromes. *Cell* 1999;97:133-44.
2. Williamson LM, Hull D, Mehta R, Reeves WG, Robinson BH, Toghill PJ. Familial Hibernian fever. *Q J Med* 1982;51(204):469-80.
3. Aksentijevich I, Galon J, Soares M, Mansfield E, Hull K, Oh HH, et al. The tumor-necrosis-factor receptor-associated periodic syndrome: new mutations in TNFRSF1A, ancestral origins, genotype-phenotype studies, and evidence for further genetic heterogeneity of periodic fevers. *Am J Hum Genet* 2001;69:301-14.
4. Aganna E, Hammond L, Hawkins PN, Aldea A, McKee SA, Ploos van Amstel HK, et al. Heterogeneity among patients with tumor necrosis factor receptor-associated periodic syndrome phenotypes. *Arthritis Rheum* 2003;48:2632-44.
5. Dode C, Andre M, Bienvenu T, Hausfater P, Pecheux C, Bienvenu J, et al. The enlarging clinical, genetic, and population spectrum of tumor necrosis factor receptor-associated periodic syndrome. *Arthritis Rheum* 2002;46:2181-8.
6. Aganna E, Martinon F, Hawkins PN, Ross JB, Swan DC, Booth DR, et al. Association of mutations in the NALP3/CIAS1/PYPAF1 gene with a broad phenotype including recurrent fever, cold sensitivity, sensorineural deafness, and AA amyloidosis. *Arthritis Rheum* 2002;46:2445-52.
7. Lachmann HJ, Papa R, Gerhold K, Obici L, Touitou I, Cantarini L, et al. The phenotype of TNF receptor-associated autoinflammatory syndrome (TRAPS) at presentation: a series of 158 cases from the Eurofever/EUROTRAPS international registry. *Ann Rheum Dis* 2014;73(12):2160-7.

8. Lobito AA, Kimberley FC, Muppidi JR, Komarow H, Jackson AJ, Hull KM, et al. Abnormal disulfide-linked oligomerization results in ER retention and altered signaling by TNFR1 mutants in TNFR1-associated periodic fever syndrome (TRAPS). *Blood* 2006;108:1320-7.
9. Omoyinmi E, Melo Gomes S, Standing A, Rowczenio DM, Eleftheriou D, Klein N, et al. Brief Report: whole-exome sequencing revealing somatic NLRP3 mosaicism in a patient with chronic infantile neurologic, cutaneous, articular syndrome. *Arthritis & rheumatology (Hoboken, NJ)* 2014;66(1):197-202.
10. Banner DW, D'Arcy A, Janes W, Gentz R, Schoenfeld HJ, Broger C, et al. Crystal structure of the soluble human 55 kd TNF receptor-human TNF beta complex: implications for TNF receptor activation. *Cell* 1993;73(3):431-45.
11. Leaver-Fay A, Tyka M, Lewis SM, Lange OF, Thompson J, Jacak R, et al. ROSETTA3: an object-oriented software suite for the simulation and design of macromolecules. *Methods Enzymol* 2011;487:545-74.
12. Willard L, Ranjan A, Zhang H, Monzavi H, Boyko RF, Sykes BD, et al. VADAR: a web server for quantitative evaluation of protein structure quality. *Nucleic Acids Res* 2003;31(13):3316-9.
13. Berjanskii M, Zhou J, Liang Y, Lin G, Wishart DS. Resolution-by-proxy: a simple measure for assessing and comparing the overall quality of NMR protein structures. *J Biomol NMR* 2012;53(3):167-80.
14. Humphrey W, Dalke A, Schulten K. VMD: visual molecular dynamics. *J Mol Graph* 1996;14(1):33-8, 27-8.
15. Touitou I, Lesage S, McDermott M, Cuisset L, Hoffman H, Dode C, et al. Infervers: an evolving mutation database for auto-inflammatory syndromes. *Hum Mutat* 2004;24(3):194-8.

16. D'Ostualdo A, Ferlito F, Prigione I, Obici L, Meini A, Zulian F, et al. Neutrophils from patients with TNFRSF1A mutations display resistance to tumor necrosis factor-induced apoptosis: pathogenetic and clinical implications. *Arthritis Rheum* 2006;54:998-1008.
17. Rohlin A, Wernersson J, Engwall Y, Wiklund L, Bjork J, Nordling M. Parallel sequencing used in detection of mosaic mutations: comparison with four diagnostic DNA screening techniques. *Hum Mutat* 2009;30(6):1012-20.
18. Tanaka N, Izawa K, Saito MK, Sakuma M, Oshima K, Ohara O, et al. High incidence of NLRP3 somatic mosaicism in patients with chronic infantile neurologic, cutaneous, articular syndrome: results of an International Multicenter Collaborative Study. *Arthritis Rheum* 2011;63(11):3625-32.
19. Koa-Wing M, Nakagawa H, Luther V, Jamil-Copley S, Linton N, Sandler B, et al. A diagnostic algorithm to optimize data collection and interpretation of Ripple Maps in atrial tachycardias. *Int J Cardiol* 2015;199:391-400.
20. de Inocencio J, Mensa-Vilaro A, Tejada-Palacios P, Enriquez-Merayo E, Gonzalez-Roca E, Magri G, et al. Somatic NOD2 mosaicism in Blau syndrome. *J Allergy Clin Immunol* 2015.

**Figure 1. Partial DNA sequence of exon 3 of *TNFRSF1A* gene.** **A)** DNA isolated from whole blood revealed the overlapping sequence of the mutant and the wild type alleles. **B)** Wild type allele **C)** Mutant allele; were amplified independently by AS-PCR. The deleted 24 nucleotides are shown in the box in panel B. **D)** Allele specific PCR showing the annealing location of each primer on the top to the wild type and the bottom to the mutant alleles of the *TNFRSF1A* gene. Top panel, the deleted sequence of 24 nucleotides from the wild type allele is shown in green. **E)** Illumina mapped reads from targeted NGS as visualized in Integrative Genomics Viewer (IGV), showing the *TNFRSF1A* c.255\_278del as black line across the white bar, red and blue lines correspond to the forward and reverse mapped DNA sequence reads. **F)** Frequency of the mutant allele in different cell subpopulations.

**Figure 2. *In silico* modeling of the extracellular domains of TNFR1.** **A)** Four CRDs of the TNFR1 extracellular region: CRD1, CRD2, CRD3 and CRD4 shown in light brown, cyan, grey and orange respectively. The location of residues Ser86\_Glu93 in the CRD2 is shown in red. **B)** Surface profile of native TNFR1 extracellular domain; **C)** – surface profile of mutated TNFR1. Red shading indicates ligand receptor-binding pocket Glu85-Cys102, blue shading - Arg106-Gly110, orange shading - Trp136- Cys143. The structural differences resulting from the eight amino acid deletion lead to the changes on the protein surface profile including the ligand receptor-binding pockets of TNFR1 extracellular domain.

**Figure 3. Low dose anakinra provided completely effective treatment of TRAPS even under the severe environmental stress of the Antarctic.** Our patient undertook a 920 mile unsupported expedition to the South Pole, pulling a 160 kg sledge containing 70 days of supplies including 40 syringes of anakinra, in an insulated container.

**Supplemental Figure 1. Influence of the Ser86\_Glu93del mutation on the tertiary structure of TNFR1 extracellular domain.** **A)** Native tertiary structure of TNFR1 extracellular domain. **B)** Tertiary structure of the variant receptor. **C)** Result of their alignment. Red color indicates the localization of rearrangements, black color -localization of mutation, orange color indicates amino acids located before and after deletion.

Analysis of the native and mutated tertiary structures of TNFR1 extracellular domain showed that the Ser86\_Glu93del mutation leads to structural rearrangements, such as: 1) transition of loop to  $\alpha$ -helix in the position PRO52 –ASN54; 2) loop -  $\beta$ -sheet in the position SER56-ILE57, which in its turn leads to elongation of  $\beta$ -sheet from position CYS58—LYS61 to SER56—LYS61; 3) loop -  $\beta$ -sheet in the positions GLN77-THR79 and CYS84, which in its turn leads to elongation of  $\beta$ -sheet from position ASP-80-CYS84 to GLN-77 – GLU83; 4) loop -  $\beta$ -sheet in the positions GLY110 – GLN111 and SER115 – SER116 which in its turn leads to elongation of  $\beta$ -sheet from position VAL112 – SER116 to GLY110 – SER115; 5) loop -  $\beta$ -sheet in the position THR123, which leads to elongation of  $\beta$ -sheet from position VAL124 – CYS127 to THR123 – CYS127; 6) loop -  $\beta$ -sheet in the positions ASN130 and SER137, which leads to elongation of  $\beta$ -sheet from GLN131 – TRP136 to ASN130 – SER137; 7) loop -  $\beta$ -sheet in the position ASN139 – LEU140, which leads to elongation of  $\beta$ -sheet from PHE141 – ASN145 to ASN139 – ASN145; 8)  $\beta$ -sheet - loop in the position

SER157, which leads to shortening of  $\beta$ -sheet from GLY152 – SER157 to GLY152 – LEU156; 9) loop -  $\beta$ -sheet in the position THR164 and  $\beta$ -sheet – loop in the positions CYS168 – HIS169, which leads to shortening of  $\beta$ -sheet from VAL165 – HIS169 to THR164 – THR167; 10) loop -  $\beta$ -sheet in the position GLY171 and  $\beta$ -sheet – loop in the position GLU176, which leads to displacement of  $\beta$ -sheet from PHE172 – GLU176 to GLY171 – ARG175; 11)  $\beta$ -sheet - loop in the positions GLU178 and CYS182, which leads to displacement of  $\beta$ -sheet from GLU178- CYS182 to ASN177 – SER181.

Accepted Article

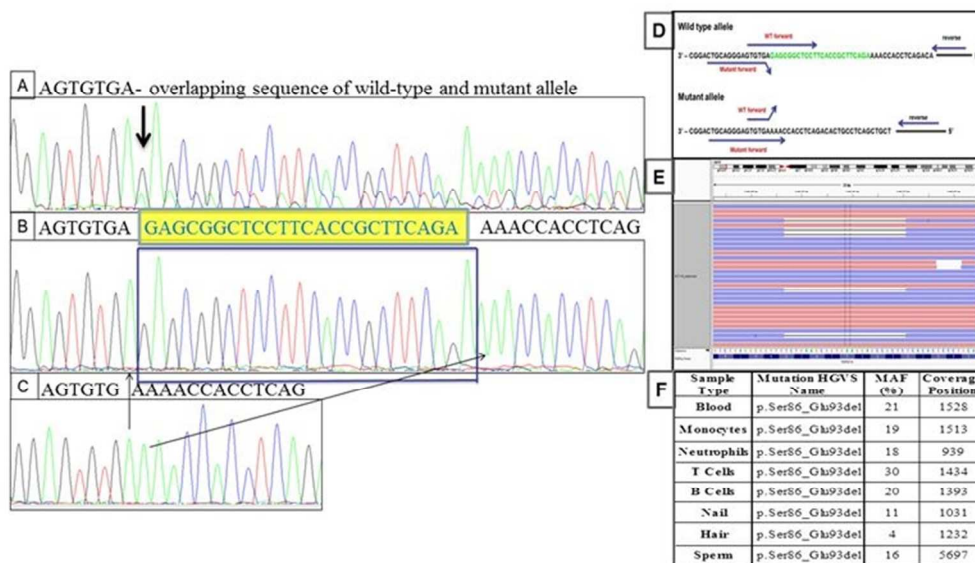


Figure 1. Partial DNA sequence of exon 3 of TNFRSF1A gene. A) DNA isolated from whole blood revealed the overlapping sequence of the mutant and the wild type alleles. B) Wild type allele C) Mutant allele; were amplified independently by AS-PCR. The deleted 24 nucleotides are shown in the box in panel B. D) Allele specific PCR showing the annealing location of each primer on the top to the wild type and the bottom to the mutant alleles of the TNFRSF1A gene. Top panel, the deleted sequence of 24 nucleotides from the wild type allele is shown in green. E) Illumina mapped reads from targeted NGS as visualized in Integrative Genomics Viewer (IGV), showing the TNFRSF1A c.255\_278del as black line across the white bar, red and blue lines correspond to the forward and reverse mapped DNA sequence reads. F) Frequency of the mutant allele in different cell subpopulations.

66x39mm (300 x 300 DPI)

Accepted

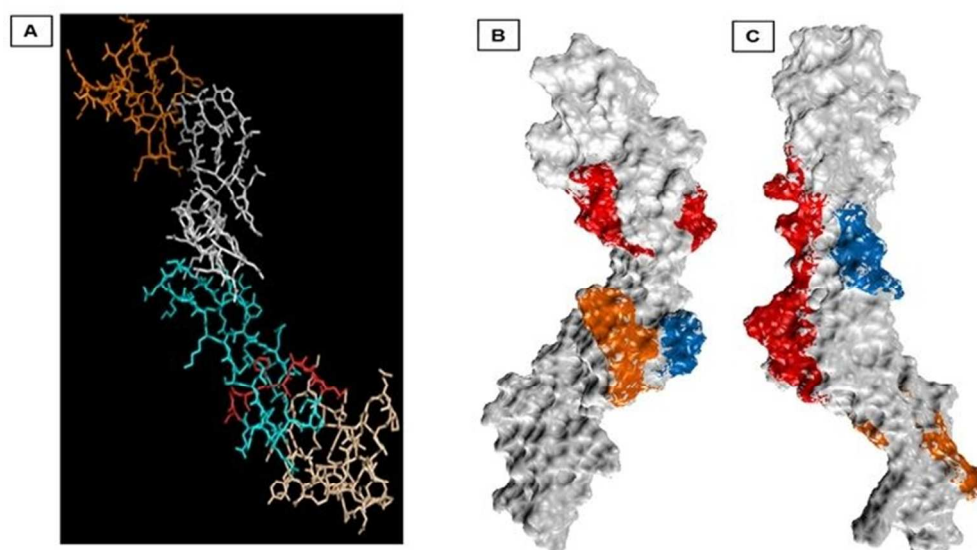


Figure 2. In silico modeling of the extracellular domains of TNFR1. A) Four CRDs of the TNFR1 extracellular region: CRD1, CRD2, CRD3 and CRD4 shown in light brown, cyan, grey and orange respectively. The location of residues Ser86\_Glu93 in the CRD2 is shown in red. B) Surface profile of native TNFR1 extracellular domain; C) – surface profile of mutated TNFR1. Red shading indicates ligand receptor-binding pocket Glu85-Cys102, blue shading - Arg106-Gly110, orange shading - Trp136- Cys143. The structural differences resulting from the eight amino acid deletion lead to the changes on the protein surface profile including the ligand receptor-binding pockets of TNFR1 extracellular domain.  
65x38mm (300 x 300 DPI)

Accept



Figure 3. Low dose anakinra provided completely effective treatment of TRAPS even under the severe environmental stress of the Antarctic. Our patient undertook a 920 mile unsupported expedition to the South Pole, pulling a 160 kg sledge containing 70 days of supplies including 40 syringes of anakinra, in an insulated container.

48x17mm (300 x 300 DPI)

Accepted